



HAL
open science

GMT Based Comparative Geomorphological Analysis of the Vityaz and Vanuatu Trenches, Fiji Basin

Polina Lemenkova

► **To cite this version:**

Polina Lemenkova. GMT Based Comparative Geomorphological Analysis of the Vityaz and Vanuatu Trenches, Fiji Basin. *Geodetski List*, 2020, 74(97) (1), pp.19 - 39. 10.6084/m9.figshare.12249773 . hal-02564526

HAL Id: hal-02564526

<https://hal.science/hal-02564526>

Submitted on 5 May 2020

HAL is a multi-disciplinary open access archive for the deposit and dissemination of scientific research documents, whether they are published or not. The documents may come from teaching and research institutions in France or abroad, or from public or private research centers.

L'archive ouverte pluridisciplinaire **HAL**, est destinée au dépôt et à la diffusion de documents scientifiques de niveau recherche, publiés ou non, émanant des établissements d'enseignement et de recherche français ou étrangers, des laboratoires publics ou privés.



Distributed under a Creative Commons Attribution 4.0 International License

GMT Based Comparative Geomorphological Analysis of the Vityaz and Vanuatu Trenches, Fiji Basin

Polina LEMENKOVA¹ – Qingdao

ABSTRACT. The study is geographically focused on the two deep-sea trenches: Vanuatu and Vityaz, Fiji Basin, East Australia, located in the area of the double convergent complex boundary of Pacific and Indo-Australian plates in the North Fiji back-arc basin. Complex geophysical settings results in the formation of the trenches, seismicity, geodynamic complexity and instability of the region. The work aimed at modelling and comparative statistical analysis of the bathymetry and geomorphology of two trenches. Technically, the methodology of this work is based on the Generic Mapping Tools (GMT) using cartographic mapping of the geophysical, tectonic and geological settings, 2D and 3D modelling, visualizing raster grids GEBCO, ETOPO1, ETOPO5. Histogram topographic equalization (equalized, normalized, quadratic) was done using module 'grdhisteq'. Modelling geoid and gravity was based on EGM96 by sequence of GMT modules. The cross-spectrals of 2D binary raster grids were compared and their coherency plotted by 'grdffr'. The automated cross-sectioning was done using 'grdtrack' module. The results include modelled transects visualizing trenches asymmetry, bathymetric and geomorphic variations. Vityaz Trench is shallower with depths <-6,100 m, has 'bell-shape' data distribution with two peaks at ranges -3,500 m to -3,700 m, and -4,800 m to -5,000 m. Vanuatu Trench reaches up to -7,000 m with majority of values between -5,000 m to -3,000 m, even data distribution with depth increasing at -2,200 m to -800 m. Geomorphic form of both trenches varies: Vityaz has flat wide bottom similar to a trough, steeper gradient eastern slope. Vanuatu has V-form classic shape with gentle shapes on both slopes. Selected segment of Vityaz has shallower depths with maximal <-5,000 m while Vanuatu is deeper (-6,000 m). Cartographic functionality of the GMT is presented by various cartographic projections: Mercator, Behrman, Cylindrical Stereographic, Hammer retroazimuthal. 3D modelling was done using GMT module 'grdview'. Trenches were visualized and rotated at 160°/45°azimuth. Presented maps, 2D and 3D models and graphics are plotted and visualized by GMT with selected code snippets explained. Current work contributes to the methods of the modelling of deep-sea trenches geomorphology.

Keywords: Vanuatu Trench, Vityaz Trench, Fiji, Pacific Ocean, GMT, cartography.

¹ Polina Lemenkova, MSc, College of Marine Geo-sciences, Ocean University of China, 238 Songling Rd., Laoshan, 266100, Qingdao, Shandong, China (P.R.C.), e-mail: pauline.lemenkova@gmail.com.

1. Introduction

1.1. Research problem and goal

The research aim is comparative geomorphic analysis of two deep-sea trenches: Vanuatu and Vityaz. The trenches are located in the geologically complex region of the southwest Pacific Ocean, Fiji, East Australia. This region is situated in the area of the double convergent plate complex boundary where Pacific Plate subducts under the Indo-Australian plate westwards, and Indo-Australian plate beneath the North Fiji back-arc basin northeastwards. Such complex geophysical settings results in formation of these trenches, and also high seismicity, geodynamic complexity and instability of this region. Besides, the region is a part of the 'Ring of Fire' bordering Pacific Ocean where active movements of the tectonic plates and volcanism take place. Therefore, additional goal was to visualize geophysical settings of the study area through series of the thematic maps. These include geophysical, geological and tectonic settings that are the most important causes of the ocean trench formation. Hence, cartographic objective of the research was to visualize bathymetry, geomorphology, tectonic and geological settings of the trenches through 2D and 3D modelling and mapping. The statistical analysis aimed to compare datasets on two trenches and highlight differences in their geomorphic and bathymetric structure (data distribution at various depths).

Technical objective of the demonstrated study was to present functionality of the Generic Mapping Tools (GMT) and to test a GMT based approaches to quantify the variability of the bathymetry in spatially distributed segments of the Vanuatu and Vityaz trenches. The approach of the profile modelling was exemplified using enlarged square of the two selected segments of the submarine topography of the Vanuatu and Vityaz trenches as modelling targets. However, the general mindset of the presented method is applicable to any other deep-sea trenches or troughs. The GMT was selected as a main instrument, due to its high functionality and Unix-compatibility (the GMT scripts are run from the console). Besides, GMT has cartographic fine solutions (variety of projections, colour palettes, layouts, data processing and modelling), and advantage of the included statistical modules.

1.2. Study area

Geography

The geographic focus of the study area is located in Fiji Basin, East Australia, two oceanic trenches: Vanuatu (a.k.a. New Hebrides) and Vityaz (Fig. 1). The Vanuatu arc stretches ca. 1200 km in the SW Pacific Ocean located in the area with coordinates 10°S–23°S, 160°–180°E (Fig. 1). Narrow Vanuatu Trench is bordered by the Vanuatu volcanic archipelago, a submersed part of an oceanic arc extending in 12° and 25°S, from Torres to Hunter Islands (Jean-Baptiste et al. 2016), 1000 km to the NW off Kermadec.

Tectonics

The origin of the New Hebrides trench-arc system is caused by the Indo-Australian subducting tectonic plate and a subduction of the d'Entrecasteaux ridge

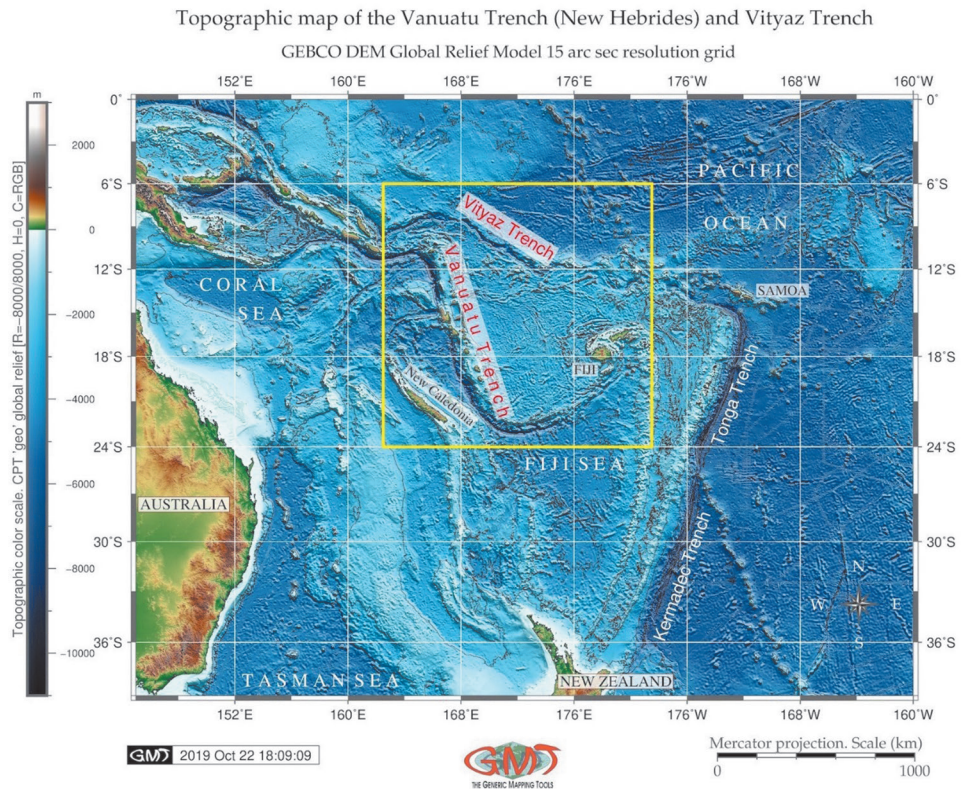


Fig. 1. *Topographic map of the Fiji Basin, East Australia.*

(Charvis and Pelletier 1989). Previous surveys on bathymetry, magnetism, seismicity and focal mechanism in the region between the southern New Hebrides Arc and North Fiji Basin enlighten the geodynamic complexity and instability of the area (Maillet et al. 1989). Tectonic development of the Vanuatu Trench has two distinct subduction stages (Jean-Baptiste et al. 2016): 1) subduction of the Pacific Plate under the Indian-Australian plate westward direction; 2) subduction of the Indo-Australian plate beneath the North Fiji back-arc basin at the margin of the Pacific Plate, north-eastwards direction. Therefore, the convergence is marked by two opposite subduction zones, defined by the Vanuatu Trench to the west and the Tonga Trench to the east, resulting in an asymmetric opening of the North Fiji back-arc basin (Auzende et al. 1995). The Vanuatu trench-arc system divides New Hebrides back-arc troughs and active North Fiji marginal basin.

Volcanism

The New Hebrides archipelago is a complex reversed-arc system that divided into four major volcanic provinces (Carney and Macfarlane 1982): 1) Western Belt is an Early Miocene extinct volcanic arc in the frontal arc; 2) The Eastern Belt formed in the Middle Miocene, a calc-alkaline arc volcanism; 3) Marginal Province

submerged in the Early Pleistocene is shown by volcanic activity; 4) The Central Chain is a present volcanic line continues Marginal Province volcanism. Currently, the New Hebrides island arc consists of numerous volcanoes that frequently form islands situated in a tectonically complex arc-backarc system (Beier et al. 2018, Calmant et al. 2003), Fig. 2. An an active volcano Mt. Yasur, is located in Tanna Island of the Vanuatu arc (Spina et al. 2016).

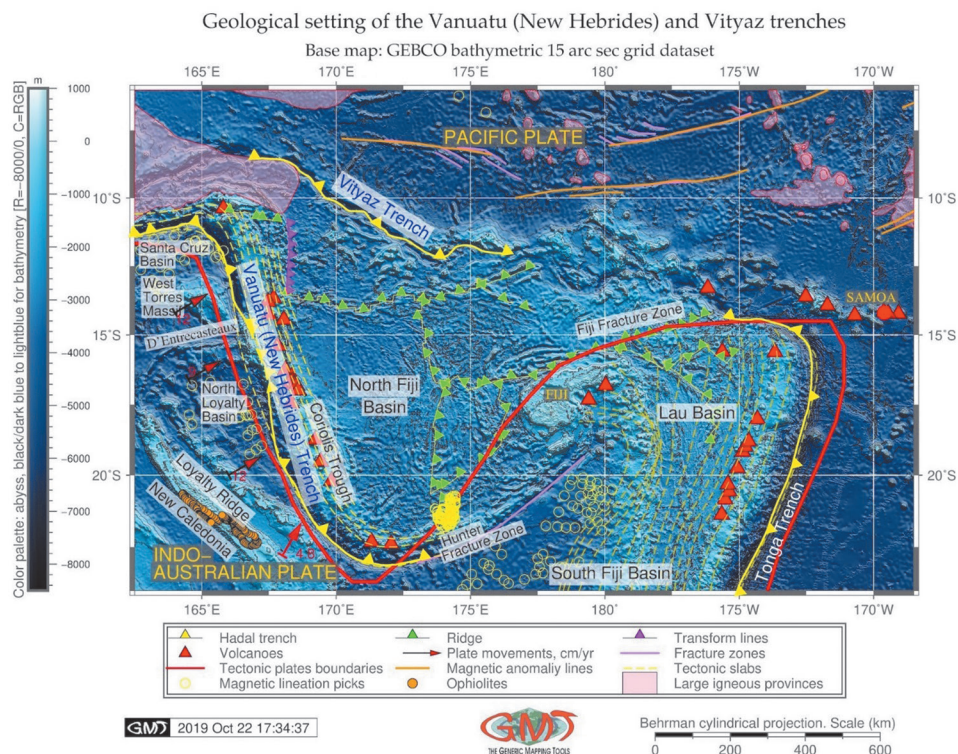


Fig. 2. Geologic map of the Fiji Basin, East Australia.

Geomorphology

The geomorphology of the Vanuatu Trench has masses of rubble, talus slopes and fragmented outcrops (Heezen and Hollister 1971), with ca. 7156 m. Relative to other neighbour trenches (Kermadec, Mariana), it is warmest, and underlies intermediate bio-productivity (Linley et al. 2017). The Vanuatu Trench has developed in a situation of complex tectonic settings. More specifically, it is located in a double convergent boundary between the Australian and Pacific tectonic plates (Beaumais et al. 2016).

The anomalous geomorphology of the central New Hebrides arc is caused by the subduction of the D'Entrecasteaux aseismic ridge which enters the central part of

the Vanuatu Trench. Besides, there is a deformation distributed over numerous spreading ridges in Lau and North Fiji back-arc basins. Geometry of Lau and North Fiji back-arc basins and segmentation of the New Hebrides arc are significantly influenced by the subduction of aseismic ridges: Louisville, D'Entrecasteaux and Loyalty (Pelletier et al. 1998) (Fig. 2).

Geology

The basaltic rocks from the central and southern islands of the New Hebrides (Aneityum, Tanna, Erromango, Efate, Emae, Tongoa and Epi), have geochemical features typical of island arc volcanics. The basalts from Futuna island located farther from the trench show features typical of calc-alkaline rocks (Dupuy et al. 1982). Three islands (Maré, Lifou and Ouvéa), mainly covered by forests and flat in relief, illustrate tectonic deformation at various distances from the Vanuatu Trench. Loyalty Islands serve as tension cracks resulting from the elastic bulging of the Australian plate before its subduction at the Vanuatu Trench (Bogdanov et al. 2011).

Further discussions on the geologic setting of the Vanuatu Trench exist in relevant literature (Monzier et al. 1997, Sorbadere et al. 2011, Turtle et al. 2016, Louat and Pelletier 1989, Bourrouilh-Le Jan and Talandier 1985, Pillet and Pelletier 2004), where particular attention is paid to geochemistry, mineralogy, magmatism, volcanology, seismicity and tectonics of the region.

2. Methods

Current paper is based on using Generic Mapping Tools (GMT) cartographic scripting toolset developed by Wessel and Smith (1998). Examples of using GMT in marine bathymetric mapping and data processing (Gauger et al. 2007, Kuhn et al. 2006) prove its cartographic functionality and effectiveness.

2.1. Histogram equalization on the topography grids

Topographic histogram equalization (Fig. 3) were plotted as 4 subplots using GMT module 'grdhisteq' used to find the data values dividing two grid files into patches of equal area. Hence, 'grdhisteq' performs sort of histogram equalization of a raster images using this code snippet: `gmt grdhisteq vt_relief.nc -Gout.nc -C16`, and for other maps: `gmt makecpt -Crainbow -T0/15/1 > c.cpt`, and `gmt makecpt -Crainbow -T0/15 > q.cpt`. More specifically, using 'grdhisteq', the ASCII list of the data values which divide the range of the initial raster data into cells segments that has been written to an output file. In this case, a -C16 argument defines 16 cells.

The resulting raster grid has an equal area in the image. Using 'makecpt' GMT module this output was then coloured using CPT by following code: `gmt makecpt -Crainbow -T11000/3000 > t.cpt`. The explanations for the subplot with four maps (Fig. 3) is as follows:

Vanuatu and Vityaz trenches: Histogram equalization on topography grid:
ETOPO1 DEM Global Relief Model 1 arc min resolution

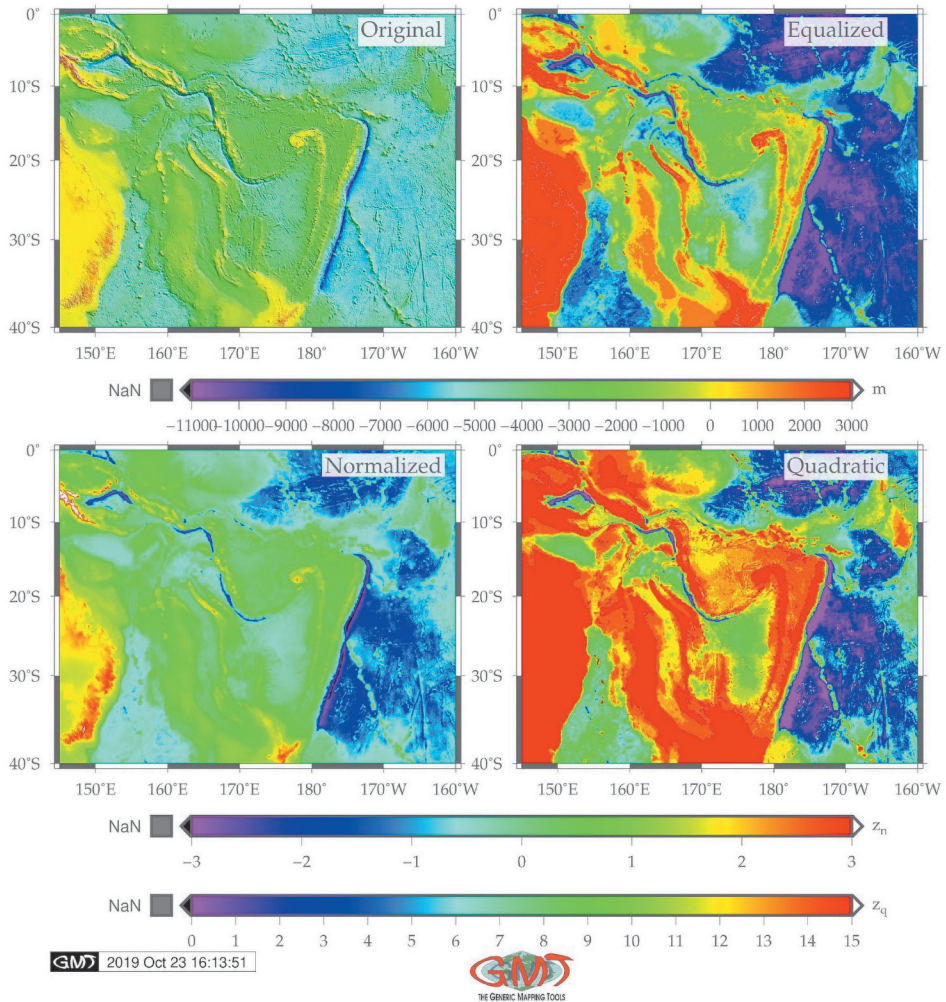


Fig. 3. Histogram equalization of the topography grids.

1. The original map (top left) shows the initial raster with applied artificial cpt 'rainbow' to highlight the changes in elevation (gmt makecpt -Crainbow -T-11000/3000 > t.cpt).

2. Second to it, (top right) is the equalized raster grid.

3. Third to it, (low left) is the normalized raster grid which was derived using -N argument that stands for Gaussian output aimed to receive data with smooth Gaussian distribution. In this case, the default standard normal scores was used for grid normalization. However, it is possible to make an output grid with scores placed within the $\langle -1, +1 \rangle$ range.

4. Finally, the fourth grid (shows low right) on Fig. 3 is a quadratic equalization that has been plotted using following code: `gmt grdhisteq vt_relief.nc -Gout.nc -Q`. Here, the '-Q' argument is output selecting quadratic histogram equalization, unlike the default linear one. Here, the '-T-11000/3000' arguments means the range of the topographic heights/depths elevations. Then, the image was visualized using 'grdimage' module using following code: `gmt grdimage vt_relief.nc -I+a45+nt1 -Ct.cpt -JM3i -Y6i -K -P -B10 -BWSne > $ps`.

In this code, the '-Ct.cpt' argument stands for the colour palette (cpt) created in the previous step, the '-JM3i' arguments explains the Mercator projection with 3 inches width; '-Y6i' argument plots the map with 6 inches distance from the previous one by Y axis; '-K' argument refers to the continuation of the code, and '-P' is a portrait orientation of the layout. The annotation was added using Unix 'echo' prog: `echo "185 -5 Original" | gmt pstext -Rvt_relief.nc -J -O -K -F+jBL+f12p -T -Gwhite10 -Dj0.1i » $ps`. Secondly, the 'grdhisteq' GMT module enables to write a raster grid with statistics based on cumulative distribution function. That means, after applying the 'grdhisteq' module, the output raster file has relative elevations in the same locations as the input file (that is, x, y). However, the values are modified to reflect their place in cumulative distribution with reference to the initial input file. This illustrates the principle of the equalization of the topographic grids by GMT module 'grdhisteq', as visualized on Fig. 3.

2.2. Modelling geophysical settings of gravity and geoid

To plot the geoid and gravity models of the Fiji Basin and Pacific/Indo-Australian plates subduction zone, the grids of the geoid and free air gravity anomalies of the region have been downloaded and extracted as a subset of img file based on the existing methodology (Lemenkova 2019j) using following GMT code snippet: `img2grd grav 27.1.img -R145/200/-39/0 -Ggrav.grd -T1 -I1 -E -S0.1 -V`. Here, the `grav 27.1.img` is the input file, the '-Ggrav.grd' defines the output file. The main module here is the 'img2grd' which reads an .img format file, extracts a subset, and converts it to .grd file.

The '-E' argument was used to force the final grid to cover the same region as requested with -R (which is a region defined by coordinates in West East South North (WESN) systems, here: 145/200/-39/0 in degrees). The final region was a direct projection of the original Mercator region extended slightly beyond the requested latitude range of Fiji Basin region: 145°200'–39°0', Fig. 4. The '-I1' indicate minutes as the width of an input img pixel in minutes of longitude, which is here equal to 1 according to the resolution. The -S0.1 GMT argument multiplies the img file values by scale before storing it in .grd file. Although the default value is 1.0, here the 0.1 was taken for the free-air gravity files in mGal*10 to get the mGal, according to the descriptions of the technical specifications of GMT (Wessel et al. 2019). The 'T1' argument of GMT type handles the encoding of constraint information. Here the '-T1' gets data values at all points, while, for instance, type = 0 would indicate that no such information is encoded in the .img file. The '-V' argument is a technical characteristics explaining the verbosity level, that is, showing the level of details in the messages reporting errors to the user/cartographer while executing the GMT script. The two grids that were operated on were first received using 'img2grd' GMT module by following code: `img2grd`

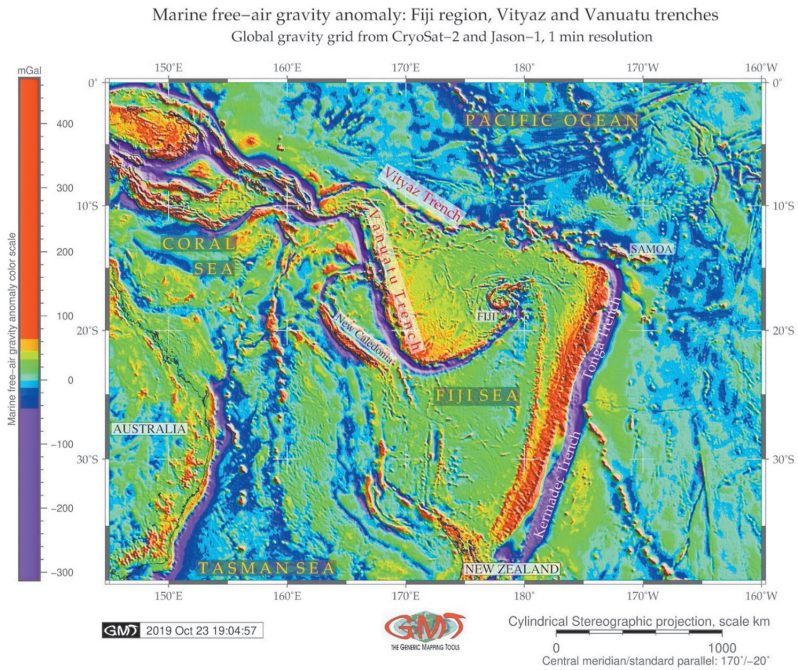


Fig. 4. Marine free-air gravity anomaly: Fiji Basin, Vanuatu and Vityaz Trenches.

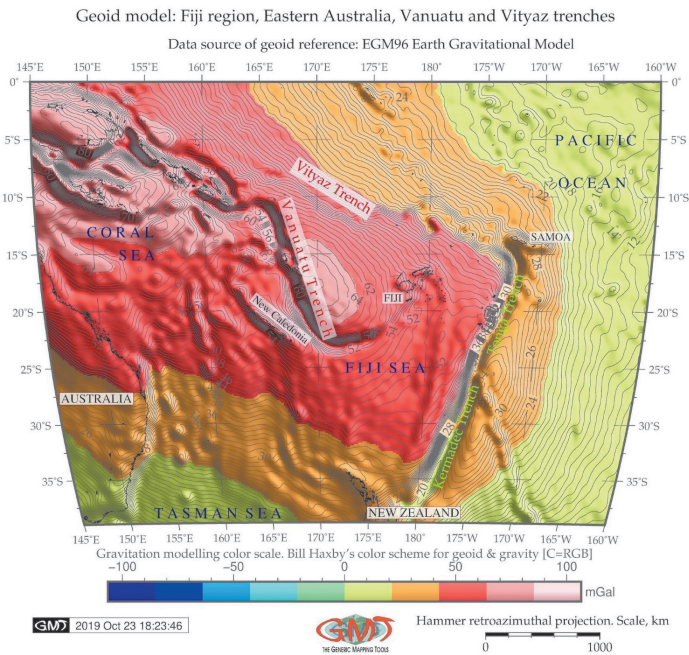


Fig. 5. Geoid model: Fiji Basin. Hammer retroazimuthal projection.

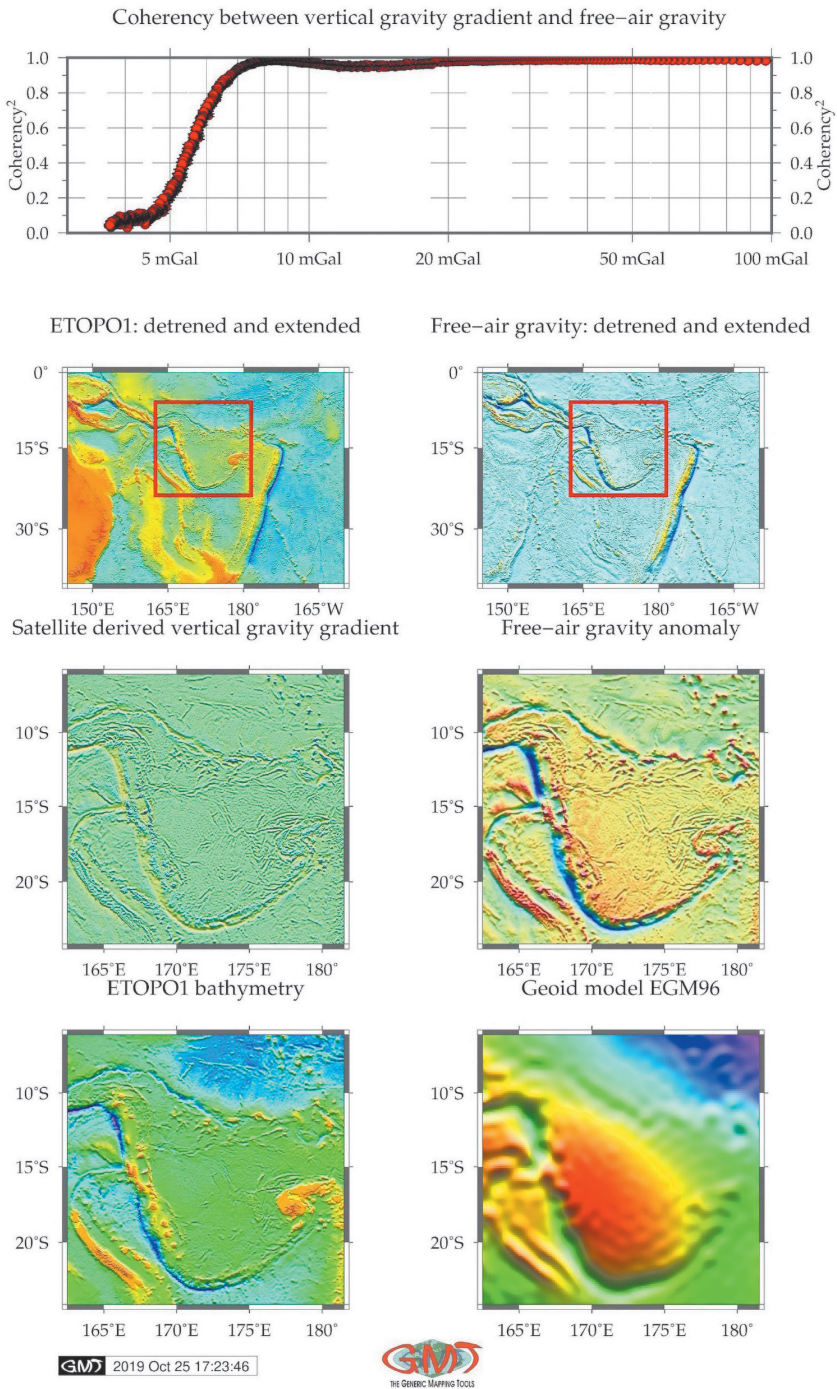


Fig. 6. Modelling coherency between marine free-air and vertical gravity anomaly.

`curv_27.1.img -R162.5/181.5/-24/-6.0 -Gvvtc_curv.grd -T1 -I1 -E -S0.01 -V` repeated for 'grav_27.1.img' file.

Afterwards, the coherency between the two grids of free-air gravity and vertical gradient was plotted using the GMT module 'grdfft' (Fig. 6). The 'grdfft' module performs mathematical operations on the grids in the wavenumber or frequency domain. The main algorithm is the following: the 'grdfft' module inputs the 2D grids to perform operations in their frequency domains using Fast Fourier Transform, and then transforms the raster grids back to the space domain using following code: `gmt grdfft vvtc_grav.grd vvtc_curv.grd -E+wk+n -Na+d+wtmp > cross_spectra.txt`. The horizontal dimensions of the grid are in m.

Here, the 'vvtc_grav.grd' and 'vvtc_curv.grd' are two 2D binary raster grids compared for cross-spectral operations (Fig. 6). The '-E' argument estimates power spectrum in the radial direction. Specifically, here the '+w' in expression '-E+wk+n' means writing wavelengths and '-k' was appended to scale wavelengths from m to km, the '+n' was appended to normalize the output so that the mean spectral values per frequency were reported. Since the '-N' argument was used with several options, brief explanations are as follows. The 'a' option was used to let 'grdfft' module to select dimensions achieving the most accurate result; the '+d' option was used to detrend data: to remove best-fitting linear trend; 'p' was used to save the polar form of magnitude to the output table; '+t' option aimed to change percentage via width while performing tapering of the data edge to the grid edge. The output grids were visualized using module 'grdimage', 'ps-basemap' and 'psxy' for coherency graph on the top of the Fig. 6. Other options are explained by Wessel et al. (2019).

2.3. 3D Modelling

The methodology of the 3D modelling using GMT module 'grdview' is described by Wessel et al. (2019). Methods were adopted for the current study with relevant coordinates using following GMT code for the Vanuatu Trench: `grdview vv3d_relief.nc -J -R -JZ4c -CrainbowVVT.cpt -p160/45 -Qsm -N- 9000+glightgray -Wm0.1p -Wf0.1p,red -Wc0.1p,magenta -B5/5/3000:"Bathymetry and topography (m)":nE-swZ -Y6.5c > $ps`. The resulting 3D models are shown on Fig. 7.

The data were initially extracted from the ETOPO5 grid using following snippet (Vanuatu Trench): `gmt grdcut earth_relief_05m.grd -R160/170/- 25/-10 -Gvv3d_relief.nc`. The ETOPO5 was selected to plot 3D to reduce the grid size and to save computer memory space. The next step of the 3D modelling is a calculation of the regular 3D grid mesh using GMT parameters of the 'grdview' module. The dimension of the grid was chosen in a way which ensures that every point of the trench axis is located within the grid boundaries. Therefore, the coordinates for Vityaz Trench were selected as 163°173°–15°0° and for the Vanuatu Trench: 160°170°–25°–10°.

Visualization parameters of the 3D models can be summarized as follows. Grid extent was in 160/45 azimuthal direction rotation with the grid ranges from 160° to 173° for both grids, latitudinal direction from –25° to 0°, vertical direction from –9,000 km depths up to 1000 km. On 'Z' argument the grid was extended by 4 cm as a visual distance between the 3D and basemap 2D, to enable interpreted them better. Data: geoid field data of the 2D map were taken from the ETOPO1 dataset (1 arc minute resolution) by following code: `gmt grdcontour earth_relief_01m.grd - J M 6.0c`

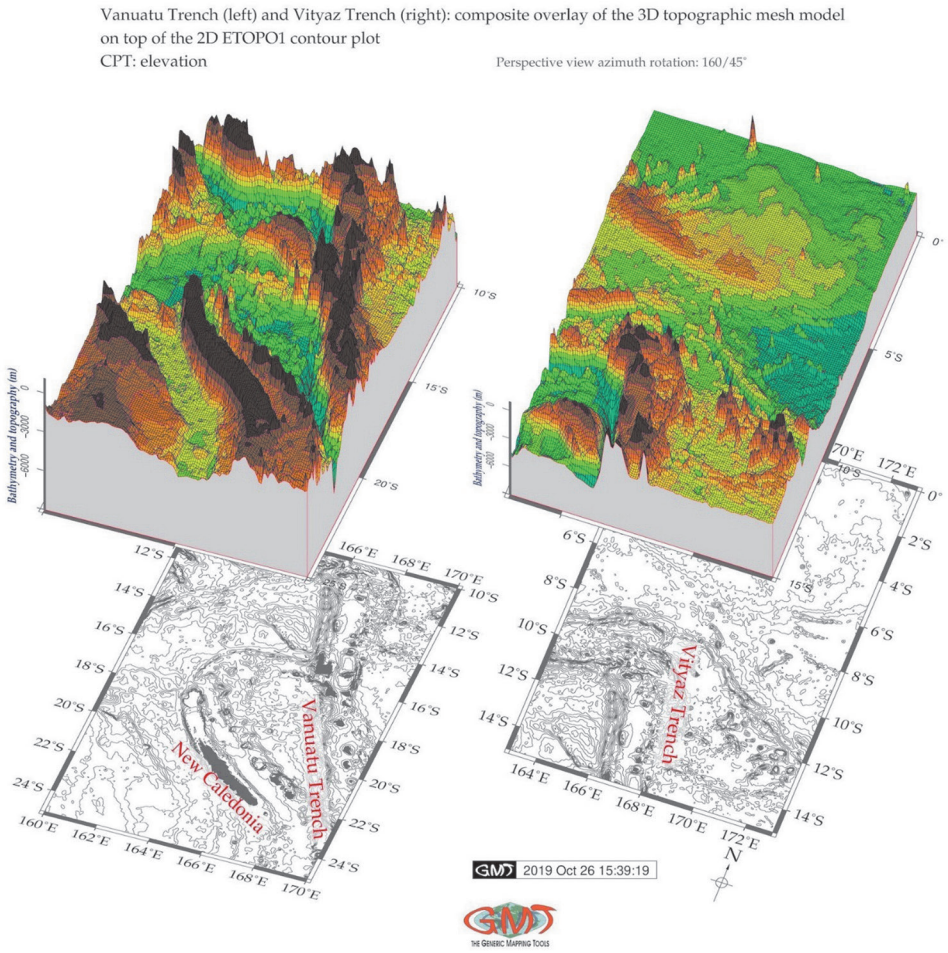


Fig. 7. 3D modelling of the Vanuatu and Vityaz Trenches.

– R160/170/ – 25/ – 10 – p160/45 – C500 – Gd6c – W thinnest, dimgray – Y 5.5c – P – K > \$ps. In order to ensure that grids are visually depict geomorphic shapes of the surfaces, the '-Qsm' argument was selected to specify 's' for the surface plot, and 'm' to have mesh lines drawn on top of surface. For the vertical component, option '-N-9000+glightgray' was selected to draw a plane at the –9,000 m level of bathymetry. Final 3D model of the two subplots is shown on Fig. 7.

2.4. Modelling geomorphic cross-section transects

Bathymetric data (depths) for samples were extracted during cross-section profiling using 'grdtrack' GMT module, which is a technique of sampling raster grids to create orthogonal cross-profiles. The methodology is adopted from the existing in technical manuals of the GMT (Wessel et al. 2019) and tested by Lemenkova (2019b).

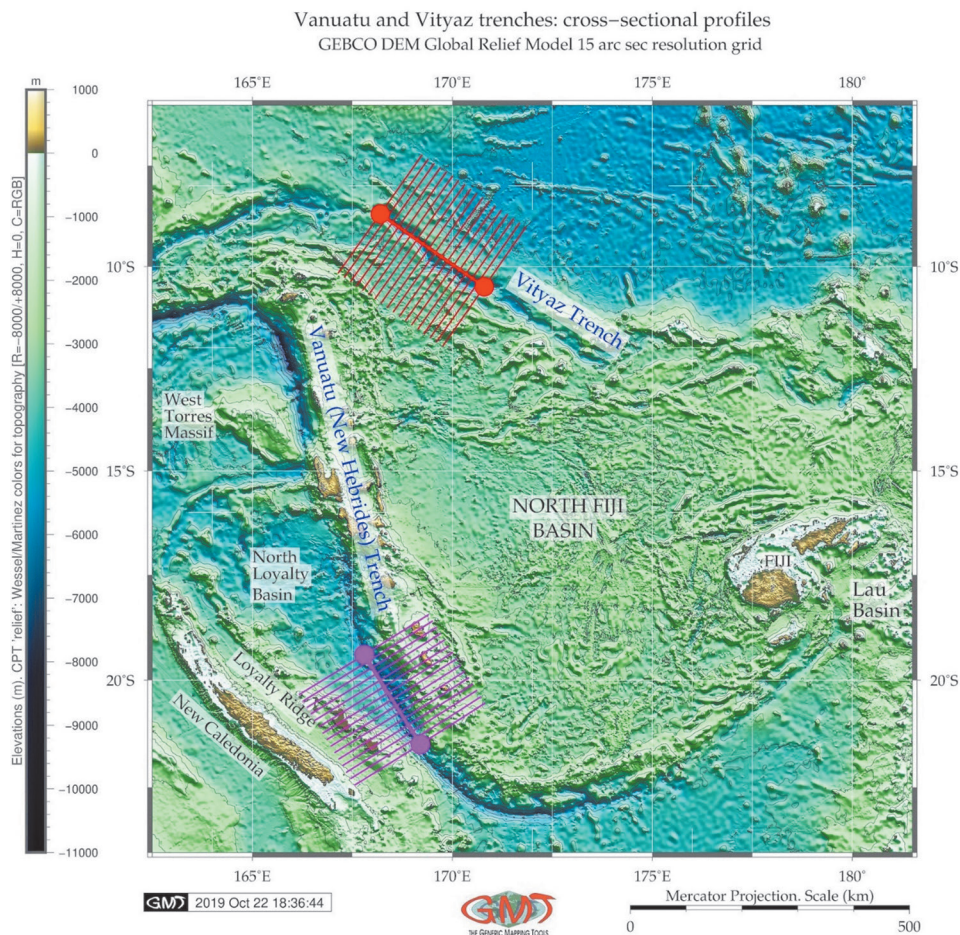


Fig. 8. Cross-section transects modelling.

Cross-section profiles were drawn across the two trench axes, 400 km long, spaced 20 km. The depths of the trenches are measured at 2 km along the profile going in a perpendicular direction at equal spacing relative to the profile length (400 km for each). These profiles were then averaged by the median values using GMT module 'grdtrack' by this code: `gmt grdtrack trenchVTs.txt -Gvvt_relief.nc -C400k/2k/20k -Sm+sstackVTs.txt > tableVTs.txt` (case of Vanuatu Trench). The shape of the trenches is highlighted as median using '-Sm' argument, red line on Fig. 9. The sampling was then repeated automatically for the whole length of the trench's selected segment (visualized on Fig. 8). Profiles were then statistically modelled to visualize median and error bars (Fig. 9, red line for median), and depths were statistically computed using 'pshistogram' GMT module. The interpolated spatial distribution of depths is a median (red line) and error bars (Fig. 9) for the extend of each trench (-200 to 200 km).

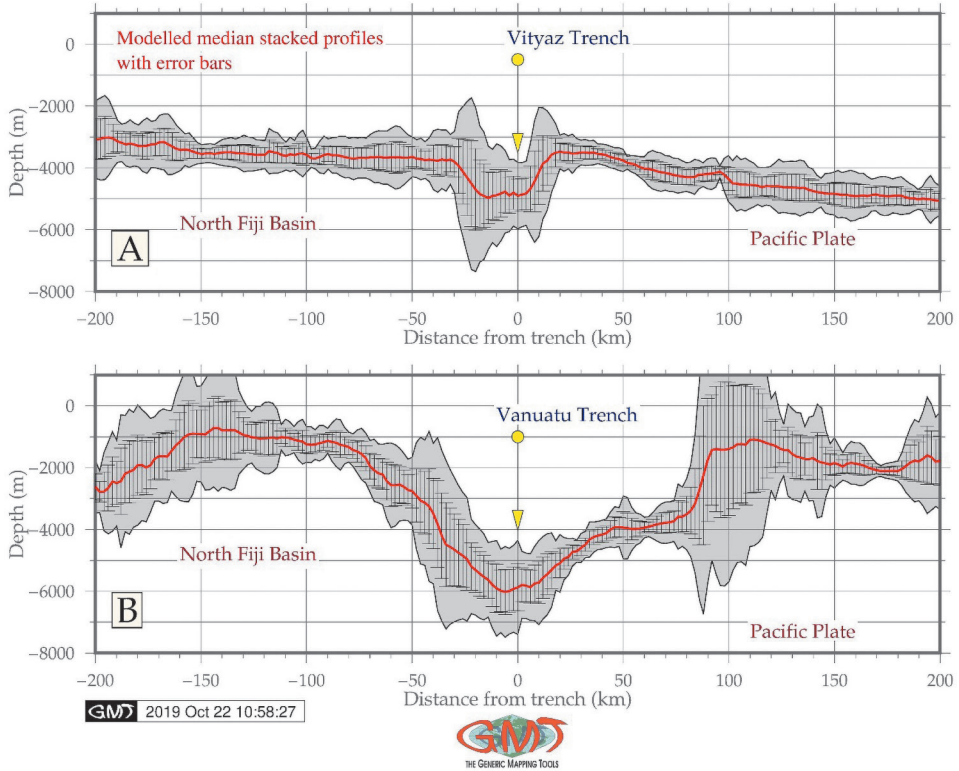


Fig. 9. Graphs showing geomorphic slope models in transects.

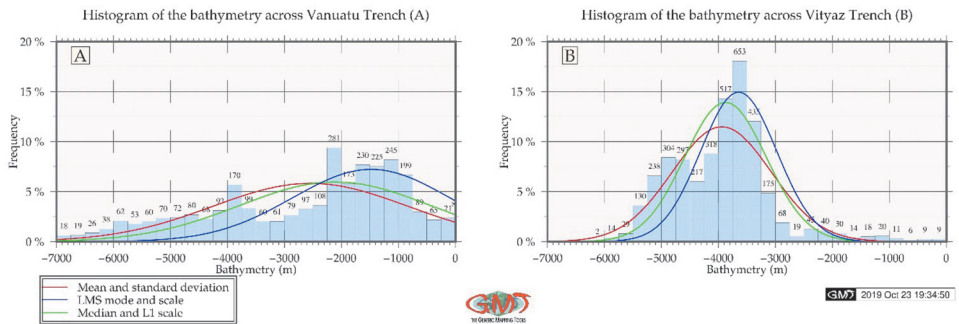


Fig. 10. Comparative statistical analysis of the Vityaz and Vanuatu Trenches.

3. Results

Topographic data used in this research include ETOPO1 and GEBCO grid containing elevation data (topography/bathymetry) for the Earth. More information about GEBCO can be further found in relevant literature (Mayer et al. 2018,

Monahan 2004, Amante and Eakins 2009) The GEBCO Gazetteer was referred to for the names of the submarine features and structures (IHO 2012). The histogram equalization on the topography grids is illustrated on Fig. 3. The satellite missions have provided marine free-air gravity and vertical gravity gradient data available for the study area and used for mapping (Fig. 4 and Fig. 5). The Earth gravitational models derived from CryoSat-2 and Jason-1 data provide marine gravity field with a spatial resolution of 1° . The gravity data from these missions (Sandwell et al. 2014) were used to visualize data and compare coherency between the marine free-air gravity and vertical gravity anomaly in the region of Fiji Basin (Fig. 6).

There are reported experiences in cartographic automatization aimed to improve and facilitate manual handmade digitizing of the bathymetric maps (Schenke and Lemenkova 2008). The GEBCO bathymetric grid was taken to model and digitize a series of the cross-section profiles along two trenches: Vityaz and Vanuatu (Fig. 8) and to plot the graphs using retrieved tables (Fig. 9). Modelling cross-section profiles for Vanuatu and Vityaz trenches demonstrated that bathymetry of the Vityaz Trench is generally shallower with depths not exceeding $-6,100$ m, while Vanuatu Trench reaches $-7,000$ m in values in the selected segment. Further comparative analysis of the geomorphic modelling of Vityaz and Vanuatu trenches results in following findings.

The geometric form of the two trenches varies: Vityaz Trench has more flat wide bottom similar to a trough, with steeper gradient slope on the eastern flank (Fig. 9, A: upper plot). On the contrary, Vanuatu Trench (Fig. 9, B: lower plot) has more V-form classic shape for the trench with gentle shapes on both western and eastern slopes. The results of the comparison of the median values (red line on Fig. 9) of two trenches furthermore show that selected segment of the Vityaz Trench has shallower depths with maximal not exceeding $-5,000$ m while Vanuatu Trench is more deep with $-6,000$ m. The deepest values $>5,000$ m for Vityaz Trench give in total 413 values (238, 130, 29, 14, 2) samples. The surrounding relief of the two trenches varies: for the case of Vityaz Trench, the neighbouring surface is rather flat while Vanuatu Trench is surrounded by more complex submarine relief of both North Fiji Basin (its eastern flank) and its western flank (Fig. 9).

Generally, a strong correlation of the trench's axes with borders of the two tectonic plates (Pacific Plate and Indo-Australian Plate) is evident. This implies that the geomorphology of the trenches is strongly correlated with slabs, since continuation of the plate movements, lineaments and extend of fracture zones leads to the formation of the trench axis strongly determined by plates motions. The geological local settings, stretch of the tectonic slabs, complex tectonic processes and sedimentation of the Vanuatu and Vityaz trenches explain differences in their structure and geomorphic shape form. Cartographic mapping and data in 2D reveal physical shape, structures and visualization of the objects, but 3D dimensional visualization is a useful addition for a visual analysis of the geomorphic shape of the objects. In view of this, local 3D model atop of the planar mode of the ETOPO1 were plotted to visualize the form and comparative view of the trenches (Fig. 7).

The statistical histograms for the transecting profiles of the Vanuatu and Vityaz trenches are visualized on Fig. 10. The evaluation of the descriptive statistics on bathymetry in Vanuatu and Vityaz trenches and interpolation approaches (Fig. 10) shows following results. Furthermore, the shape of the histogram varies by

two trenches: Vityaz Trench has a 'bell-shape' data distribution with two peaks at range $-3,500$ to $-3,700$ m, and the second at $-4,800$ to $-5,000$ m, that is the majority of values are in general within the range of $-5,000$ to $-3,000$ m. Here, there are 1605 samples (517, 653 and 435) recorded at the first peak with depth values from $-3,300$ to $-4,000$ and 839 sample observations (238, 304, 297) at depths from $-4,500$ to $-5,200$ m. The data distribution for the Vanuatu Trench is more even with slight increase of depth in the range of $-2,200$ to -800 m with total 1,353 samples recorded (281, 173, 230, 225, 245, 199 for the relevant bins on the histogram left), Fig. 10.

Cartographic functionality of GMT is assessed by the projections. In this study, four various cartographic projections were used for plotting maps: Mercator (Fig. 1, Fig. 3, Fig. 6 and Fig. 7), Behrman cylindrical (Fig. 2), Cylindrical Stereographic (Fig. 4), Hammer retroazimuthal (Fig. 5). More detailed descriptions of the technical specifications of the projections can be find in further references (Snyder 1993). The comparative analysis of the geophysical grids revealed structural characteristics of the two oceanic trenches, Vanuatu and Vityaz and adjacent oceanic crust of the north Fiji Basin. The coherency of the grids using gravity and vertical gravity gradient data confirms that the grids coincides well starting values of 10 mGal with the 3 to 10 meal gravity anomaly transition zone where the coherence increases. In the interval of 10 to 20 mGal the coherency declines to a very narrow interval, and correlation coincides until 100 mGal of the tested values. The gravity gradient coherency add new information to the interpretation of geodata covering active convergent margins in Southwest Pacific Ocean.

4. Discussions

The asymmetry of the hadal trenches reflects a phenomenon of tectonic plates subduction. Thus, as one plate bends down to the Earth's mantle, another plate is being deformed filling the growing empty space. The depths of trenches are influenced by many processes and factors controlling their actual shape and structure (Lemenkova 2018c). Correlation between the geophysical setting and geomorphology of the oceanic trenches at the seafloor confirms that tectonic plates movements and slab geometry may be the main controlling factors of the form, gradient steepness and depths of the trench cross-section profiles (Lemenkova 2018a). Other factors include s tectonics, sedimentation and geological settings. A variety of factors directly affect trench geomorphology and bathymetry: age and convergence rate of the plates, intermediate slab dip, width of the sinking plate (Stern 2005).

The motion of the oceanic plates is related to the subduction of cold and dense oceanic material into the mantle (Faccenna et al. 2007). Tectonic plates bounded by subduction zones move faster, as slabs strongly determine plate motions in two mechanisms (Conrad and Lithgow-Bertelloni 2002): either plates are pulled directly toward trenches by slabs or plates are indirectly dragged by mantle circulation triggered by the subducting lithosphere. As a result of these complex tectonic processes, the trench is being directly affected and, as a result, its geomorphology acquires its current form. This brief sketch of the oceanic trench formation illustrates the complexity of its geomorphic development until it reaches actual form. Moreover, understanding its form and shape is being complicated by its inaccessibility: deep-sea trenches are the least accessible places of the Earth that can only

be studied by indirect methods of modelling, remote sensing tool and advanced methods of data analysis without direct field observations.

The approaches to the data analysis, visualization and geological modelling are diverse. To mention some of these various approaches: tomographic, seismic and bathymetric 2D and 3D modelling, geologic cross-sectioning, seismic cross-section profiling, R programming language for analysis of correlation between variables (Lacey et al. 2018, Lemenkova 2019g), ArcGIS base assessment and calculation of measured data (Lemenkova et al. 2012), Python statistical libraries, such as Matplotlib, NumPy, SciPy, Seaborn, Pandas, StatsModels (e.g. Lemenkova 2019e). Using various software for statistical analysis of geodata can be illustrated by SPSS (Lemenkova 2019d), Gretl or GnuPlot (Lemenkova 2011). In view of a variety of the approaches and methods illustrated above, the advantage of the GMT consists in its embedded statistical module that enable to visualize data and to perform descriptive statistical visualization and modelling as histograms showing data distribution.

5. Conclusions

Submarine geomorphology forms include among others seamount chains, continental plateaus, volcanic ridges, arcs, etc. (Burbank and Anderson 2001). The Pacific Ocean is notable for its geographic immense size and impressive bathymetric expanse (165.2M km² size), its deep seafloor (mean depth 4280 m) and highly variable biological surface productivity (Linley et al. 2017). The Pacific Ocean seafloor is covered by a series of geomorphic forms whose origin is presently still discussed. This has motivated current study that involved a series of thematic maps and models of the Vanuatu trench aimed at better understanding of its geomorphology.

Presented research is directed toward better understanding geophysical, geological and geomorphic settings of the Vanuatu and Vityaz Trenches in their cross-sections, as well as technical aspects of mapping using GMT. The 3D and 2D models and statistical analysis on the bathymetry address in addition the question of topographic variations of the trench in its different parts caused by the tectonic slab dips and seismic activity in the southwest Pacific Ocean, Fiji regions. Technically, the research contributed to the development of the cartographic methods and demonstrated tested functionality of the GMT toolset.

The advantages of the GMT, demonstrated in this study, consist not only in the advanced scripting approaches but in embedded statistical analysis that enables to plot graphs directly using GMT. Statistical data processing and assessment is a crucial part in the data analysis of the geoscience research aimed to visualize and highlight trends and correlations between phenomenas and variables. Examples of geostatistical modelling are diverse: maximum intersection (MAXI) method and 3D simulation technique for earthquakes modelling (Theunissen et al. 2012); agglomerative hierarchical clustering using R libraries (Herod et al. 2016, Lemenkova 2018b, Lemenkova 2019c); similarity matrixes (Nunoura et al. 2015); regression analysis of data for visualizing their correlation or difference (Abrehdary and Sjöberg 2019, Lemenkova 2019a, Lemenkova 2019f, Marchese et al. 2017). Comparing to these approaches, the convenience of the GMT consists in its embedded

modules for statistical data interpretation (histograms, diagrams), that is, the data can be processed directly in GMT rather than converting them to the special statistical program as visualized on Fig. 10.

The study contributes towards the development of the bathymetric modelling and cartographic mapping using GMT. In contrast to the ArcGIS based traditional approaches to the cartographic visualization and mapping (Suetova et al. 2005, Klaučo et al. 2013, Klaučo et al. 2014, Klaučo et al. 2017), the GMT is notable for its scripting based approach. Based on the presented GMT methodology, the algorithm for geomorphic modelling and assessment of the trench's bathymetry using method of cross-section profiling provides a functional GMT-based framework for mapping and modelling raster data aimed at understanding and diagnosing how submarine geomorphology of the oceanic trench vary in its different segments.

ACKNOWLEDGEMENT. This research was funded by the China Scholarship Council, State Oceanic Administration, Marine Scholarship of China, Grant Nr. 2016SOA002, China.

References

- Abrehdary, M., Sjöberg, L. E. (2019): Recovering Moho constituents from satellite altimetry and gravimetric data for Europe and surroundings, *Journal of Applied Geodesy*, 13, 4, 291–303.
- Amante, C., Eakins, B. W. (2009): ETOPO1 1 Arc-Minute Global Relief Model: Procedures, Data Sources and Analysis, NOAA Technical Memorandum, 19.
- Auzende, J. M., Pelletier, B., Eissen, J. P. (1995): The North Fiji Basin: geology, structure and geodynamic evolution, In: Taylor, B. (Ed.), *Back-arc Basin: Tectonics and Magmatism*, New York, 139–175.
- Beaumais, A., Bertrand, H., Chazot, G., Dosso, L., Robin, C. (2016): Temporal magma source changes at Gaua volcano, Vanuatu island arc, *Journal of Volcanology and Geothermal Research*, 322, 30–47.
- Beier, C., Brandl, P. A., Lima, S. M., Haase, K. M. (2018): Tectonic control on the genesis of magmas in the New Hebrides arc (Vanuatu), *Lithos*, 312–313, 290–307.
- Bogdanov, I., Huaman, D., Thovert, J.-F., Genthon, P., Adler, P. M. (2011): Tectonic stresses seaward of an aseismic ridge-Trench collision zone, A remote sensing approach on the Loyalty Islands, SW Pacific, *Tectonophysics*, 499, 77–91.
- Bourrouilh-Le Jan, F. G., Talandier, J. (1985): Sédimentation et fracturation de haute énergie en milieu récifal: tsunamis, ouragans et cyclones et leur effets sur la sédimentologie et la géomorphologie d'un atoll: motu et hoa, à Rangiroa, Tuamotu, Pacifique SE, *Marine Geology*, 67, 263–333.
- Burbank, D. W., Anderson, R. S. (2001): *Tectonic Geomorphology*, Blackwell, Oxford.
- Calmant, S., Pelletier, B., Lebellegard, P., Bevis, M., Taylor, F. W., Phillips, D. A. (2003): New insights on the tectonics along the New Hebrides subduction zone based on GPS results, *Journal of Geophysical Research*, 108, 22.
- Carney, J. N., Macfarlane, A. (1982): Geological evidence bearing on the Miocene to Recent structural evolution of the New Hebrides arc, *Tectonophysics*, 87, 1–4, 147–175.

- Charvis, P., Pelletier, B. (1989): The northern New Hebrides back-arc troughs: history and relation with the North Fiji basin, *Tectonophysics*, 170, 3–4, 259–277.
- Conrad, C. P., Lithgow-Bertelloni, C. (2002): How mantle slabs drive plate tectonics, *Science*, 298, 207–209.
- Dupuy, C., Dostal, J., Marcelot, G. (1982): Geochemistry of basalts from central and southern New Hebrides arc: implication for their source rock composition, *Earth and Planetary Science Letters*, 60, 2, 207–225.
- Faccenna, C., Heuret, A., Funicello, F., Lallemand, S., Becker, T. W. (2007): Predicting trench and plate motion from the dynamics of a strong slab, *Earth and Planetary Science Letters*, 257, 29–36.
- Gauger, S., Kuhn, G., Gohl, K., Feigl, T., Lemenkova, P., Hillenbrand, C. (2007): Swath-bathymetric mapping, In: Gohl, K., *The expedition ANTARKTIS-XXIII/4 of the Research Vessel 'Polarstern' in 2006, Reports on Polar and Marine Research*, 557, 38–45.
- Heezen, B. C., Hollister, C. D. (1971): *The face of the deep*, Oxford University Press, New York.
- Herod, M. N., Li, T., Pellerin, A., Kieser, W. E., Clark, I. D. (2016): The seasonal fluctuations and accumulation of iodine-129 in relation to the hydrogeochemistry of the Wolf Creek Research Basin, a discontinuous permafrost watershed, *Science of the Total Environment*, 569–570, 1212–1223.
- IHO (2012): *GEBCO Gazetteer of Undersea Feature Names*, IHO-IOC.
- Jean-Baptiste, P., Allard, P., Fourre, E., Bani, P., Calabrese, S., Aiuppa, A., Gauthier, P. J., Parello, F., Pelletier, B., Garaebiti, E. (2016): Spatial distribution of helium isotopes in volcanic gases and thermal waters along the Vanuatu (New Hebrides) volcanic arc, *Journal of Volcanology and Geothermal Research*, 322, 20–29.
- Klaučo, M., Gregorová, B., Stankov, U. et al. (2013): Determination of ecological significance based on geostatistical assessment: a case study from the Slovak Natura 2000 protected area, *Central European Journal of Geosciences*, 5, 1, 28–42.
- Klaučo, M., Gregorová, B., Stankov, U., Markovic, V., Lemenkova, P. (2014): Landscape metrics as indicator for ecological significance: assessment of Sitno Natura 2000 sites, Slovakia, In: *Ecology and Environmental Protection, Proceedings of the Int'l Conference (BSU, March 19–20, 2014)*, Minsk, Belarus, BSU Press, 85–90.
- Klaučo, M., Gregorová, B., Koleda, P., Stankov, U., Markovic, V., Lemenkova, P. (2017): Land planning as a support for sustainable development based on tourism: A case study of Slovak Rural Region, *Environmental Engineering and Management Journal*, 2, 16, 449–458.
- Kuhn, G., Hass, C., Kober, M., Petitat, M., Feigl, T., Hillenbrand, C. D., Kruger, S., Forwick, M., Gauger, S., Lemenkova, P. (2006): The response of quaternary climatic cycles in the South-East Pacific: development of the opal belt and dynamics behavior of the West Antarctic ice sheet, *Expeditionsprogramm Nr. 75 ANT XXI-II/4*, AWI, Bremerhaven, Germany.
- Lacey, N. C., Mayor, D. J., Linley, T. D., Jamieson, A. J. (2018): Population structure of the hadal amphipod *Bathycallisoma (Scopelochirus) T schellenbergi* in the Kermadec Trench and New Hebrides Trench, SW Pacific, *Deep-Sea Research Part II*, 155, 50–60.
- Lemenkova, P. (2011): *Seagrass Mapping and Monitoring Along the Coasts of Crete, Greece*, M.Sc. Thesis, University of Twente, Faculty of Earth Observation and Geoinformation, Netherlands.

- Lemenkova, P., Promper, C., Glade, T. (2012): Economic Assessment of Landslide Risk for the Waidhofen a.d. Ybbs Region, Alpine Foreland, Lower Austria, Protecting Society through Improved Understanding, 11th Int'l Symposium on Landslides and the 2nd North American Symposium on Landslides & Engineered Slopes (NASL), Banff, Canada, 279–285.
- Lemenkova, P. (2018a): R scripting libraries for comparative analysis of the correlation methods to identify factors affecting Mariana Trench formation, *Journal of Marine Technology and Environment*, 2, 35–42.
- Lemenkova, P. (2018b): Hierarchical Cluster Analysis by R language for Pattern Recognition in the Bathymetric Data Frame: a Case Study of the Mariana Trench, Pacific Ocean, Virtual Simulation, Prototyping and Industrial Design, *Proceedings of the 5th Int'l Conference*, 2, 5, 147–152.
- Lemenkova, P. (2018c): Factor Analysis by R Programming to Assess Variability Among Environmental Determinants of the Mariana Trench, *Turkish Journal of Maritime and Marine Sciences*, 4, 146–155.
- Lemenkova, P. (2019a): Scatterplot Matrices of the Geomorphic Structure of the Mariana Trench at Four Tectonic Plates (Pacific, Philippine, Mariana and Caroline): a Geostatistical Analysis by R, *Problems of Tectonics of Continents and Oceans, Proceedings of the 51st Tectonics Meeting*, RAS Institute of Geology, GEOS, Moscow, 1, 347–352.
- Lemenkova, P. (2019b): An Empirical Study of R Applications for Data Analysis in Marine Geology, *Marine Science and Technology Bulletin*, 8, 1, 1–9.
- Lemenkova, P. (2019c): Processing oceanographic data by Python libraries NumPy, SciPy and Pandas, *Aquatic Research*, 2, 73–91.
- Lemenkova, P. (2019d): Testing Linear Regressions by StatsModel Library of Python for Oceanological Data Interpretation, *Aquatic Sciences and Engineering*, 34, 51–60.
- Lemenkova, P. (2019e): Regression Models by Gretl and R Statistical Packages for Data Analysis in Marine Geology, *International Journal of Environmental Trends*, 3, 1, 39–59.
- Lemenkova, P. (2019f): Numerical Data Modelling and Classification in Marine Geology by the SPSS Statistics, *International Journal of Engineering Technologies*, 5, 2, 90–99.
- Lemenkova, P. (2019g): Statistical Analysis of the Mariana Trench Geomorphology Using R Programming Language, *Geodesy and Cartography*, 45, 2, 57–84.
- Lemenkova, P. (2019h): K-means Clustering in R Libraries {cluster} and {factoextra} for Grouping Oceanographic Data, *International Journal of Informatics and Applied Mathematics*, 2, 1, 1–26.
- Linley, T. D., Stewart, A. L., McMillan, P. J., Clark, M. R., Geringer, M. E., Drazen, J. C., Fujii, T., Jamieson, A. J. (2017): Bait attending fishes of the abyssal zone and hadal boundary: Community structure, functional groups and species distribution in the Kermadec, New Hebrides and Mariana trenches, *Deep-Sea Research Part I*, 121, 38–53.
- Louat, R., Pelletier, B. (1989): Seismotectonics and present-day relative plate motions in the New Hebrides, North Fiji Basin region, *Tectonophysics*, 167, 41–55.
- Maillet, P., Monzier, M., Eissen, J.-P., Louat, R. (1989): Geodynamics of an arc-ridge junction: the case of the New Hebrides Arc/North Fiji Basin, *Tectonophysics*, 165, 1–4, 251–258, 261–268.

- Marchese, E., Scorpio, V., Fuller, I., Mccoll, S., Comiti, F. (2017): Morphological changes in Alpine rivers following the end of the Little Ice Age, *Geomorphology*, 295, 811–826.
- Monzier, M., Robin, C., Eissen, J.-P., Cotten, J. (1997): Geochemistry vs. seismo-tectonics along the volcanic New Hebrides Central Chain (Southwest Pacific), *Journal of Volcanology and Geothermal Research*, 78, 1–29.
- Nunoura, T., Takaki, Y., Hirai, M., Shimamura, S., Makabe, A., Koide, O., Kikuchi, T., Miyazaki, J., Koba, K., Yoshida, N., Sunamura, M., Takai, K. (2015): Hadal biosphere: Insight into the microbial ecosystem in the deepest ocean on Earth, *Proceedings of the National Academy of Sciences (PNAS)*, 112, 11, E1230–E1236.
- Pelletier, B., Calmant, S., Pillet, R. (1998): Current tectonics of the Tonga–New Hebrides region, *Earth and Planetary Science Letters*, 164, 263–276.
- Pillet, R., Pelletier, B. (2004): Tectonique active, tsunamis et sismicité en Nouvelle Calédonie, *Notes Techniques, Sciences de la Terre, Géologie-Géophysique, IRD Noumea*, 28, 19 p., mise à jour 2005.
- Schenke, H. W., Lemenkova, P. (2008): Zur Frage der Meeresboden-Kartographie: Die Nutzung von AutoTrace Digitizer für die Vektorisierung der Bathymetrischen Daten in der Petschora-See, *Hydrographische Nachrichten*, 25, 81, 16–21.
- Snyder, J. P. (1993): *Flattening the Earth: Two Thousand Years of Map Projections*, University of Chicago Press, Chicago, 15, 228–229.
- Sorbadere, F., Schiano, P., Metrich, N., Garaebiti, E. (2011): Insights into the origin of primitive silica-undersaturated arc magmas of Aoba volcano (Vanuatu arc), *Contributions to Mineralogy and Petrology*, 162, 995–1009.
- Spina, L., Taddeucci, J., Cannata, A. (2016): Explosive volcanic activity at Mt. Yasur: A characterization of the acoustic events, (9–12th July 2011), *Journal of Volcanology and Geothermal Research*, 322, 175–183.
- Stern, R. J. (2005): Ocean Trenches, Reference Module in Earth Systems and Environmental Sciences, *Encyclopedia of Geology, Tectonics*, 428–437.
- Suetova, I. A., Ushakova, L. A., Lemenkova, P. (2005): Geoinformation mapping of the Barents and Pechora Seas, *Geography and Natural Resources*, 4, 138–142.
- Theunissen, T., Font, Y., Lallemand, S., Gautier, S. (2012): Improvements of the Maximum Intersection Method for 3D Absolute Earthquake Locations, *Bulletin of the Seismological Society of America*, 102, 4, 1764–1785.
- Turtle, E. P., Lopes, R. M. C., Lorenz, R. D. (2016): Temporal behavior and temperatures of Yasur volcano, Vanuatu from field remote sensing observations, May 2014, *Journal of Volcanology and Geothermal Research*, 322, 158–167.
- Wessel, P., Smith, W. H. F. (1998): New, improved version of the generic mapping tools released, *EOS Transactions American Geophysical Union*, 79, 579.
- Wessel, P., Smith, W. H. F., Scharroo, R., Luis, J., Wobbe, F. (2019): *The Generic Mapping Tools, GMT Man Pages, Release 5.4.5 [Computer software manual]*, U.S.A.

Komparativna geomorfološka analiza brazdi Vityaz i Vanuatu, Fidži bazen, na osnovi GMT-a

SAŽETAK. Studija je geografski orijentirana na dvije duboko-morske brazde: Vanuatu i Vityaz, Fidži bazen, Istočna Australija, smještene u području dvostruko konvergentne kompleksne granice između Pacifičke i Indo-australske ploče u stražnjem luku bazena u Sjevernom Fidžiju. Kompleksni geofizički smještaj rezultira stvaranjem brazdi, seizmičnošću, geodinamičnom kompleksnošću i nestabilnošću regije. Cilj je rada modeliranje i komparativna statistička analiza batimetrije i geomorfologije dviju brazdi. Metodologija ovog rada se tehnički temelji na Generic Mapping Tools (GMT) koristeći kartografsko prikazivanje geofizičke, tektonske i geološke građe, 2D i 3D modeliranje te vizualizaciju rasterskih mreža GEBCO, ETOPO1 i ETOPO5. Topografsko izjednačavanje histograma (izjednačen, normaliziran, kvadratni) izvedeno je primjenom modula 'grdhisteq'. Modeliranje geoida i gravitacije temeljeno je na EGM96 po nizu GMT modula. Unakrsne spektralne linije 2D binarnih rasterskih mreža bile su uspoređene te je njihova koherentnost ucrtana pomoću 'grdff'. Automatski poprečni presjek napravljen je pomoću modula 'grdtrack'. Rezultati uključuju modelirane presjeka koji vizualiziraju asimetričnost brazdi, batimetrijske i geomorfološke varijacije. Brazda Vityaz je plića s dubinama <-6100 m, ima raspodjelu podataka u 'obliku zvona' s dva vrha u rasponu od -3500 m do -3700 m te od -4800 m do -5000 m. Brazda Vanuatu proteže se do -7000 m s većinom vrijednosti od -5000 m do -3000 m, ujednačenom raspodjelom podataka s dubinom koja se povećava na -2200 m do -800 m. Geomorfološki oblik obiju brazdi varira: brazda Vityaz ima plosnato široko dno slično koritu, strmiji gradijent istočne kosine. Brazda Vanuatu ima klasični oblik slova V s blagim oblicima na objema kosinama. Odabrani segment brazde Vityaz ima pliće dubine s maksimalno <-5000 m dok je brazda Vanuatu dublja (-6000 m). Kartografska funkcionalnost GMT-a prikazana je u različitim kartografskim projekcijama: Mercatorova, Behrmanova, cilindrična stereografska, retroazimutalna Hammerova. 3D modeliranje je napravljeno primjenom GMT modula 'grdview'. Brazde su vizualizirane i rotirane pod azimutom 160°/45°. Prikazane karte, 2D i 3D modeli te grafika iscertani su i vizualizirani primjenom GMT-a s objašnjenjem odabranih kodnih isječaka. Ovaj rad daje doprinos metodama modeliranja geomorfologije duboko-morskih brazdi.

Ključne riječi: brazda Vanuatu, brazda Vityaz, Fidži, Tihi ocean, GMT, kartografija.

Received / Primljeno: 2020-01-29

Accepted / Prihvaćeno: 2020-03-09